

Simultaneous density and magnetic field fluctuation measurements by far-infrared interferometry and polarimetry in MST^{a)}

T. F. Yates, W. X. Ding, T. A. Carter, and D. L. Brower

Department of Physics and Astronomy, University of California Los Angeles, Los Angeles, California 90095, USA

(Presented 13 May 2008; received 12 May 2008; accepted 14 July 2008; published online 31 October 2008)

Fluctuations are expected to play an important role in anomalous particle, momentum, and energy transport for magnetic confinement devices. Magnetic and density fluctuations are simultaneously measured using a high-speed laser-based Faraday rotation-interferometry system with a bandwidth of 500 kHz and 8 cm chord spacing. Density fluctuation and magnetic fluctuation profiles are obtained by using a newly developed fitting procedure. © 2008 American Institute of Physics.

[DOI: 10.1063/1.2966377]

I. INTRODUCTION

Fluctuation-induced transport in a magnetically confined plasma continues to be a topic of great interest to the fusion community. Anomalous particle transport arises from the correlated product of density fluctuations and radial velocity fluctuations. Radial velocity fluctuations can result from either electrostatic or magnetic fluctuations.¹⁻⁴ Magnetic fluctuation-induced particle transport is of particular importance for the reversed-field pinch (RFP) where global tearing instabilities driven by the current density gradient can cause magnetic field lines to wander stochastically in space. Plasma displacement associated with magnetic perturbations will result in density fluctuations as well. To understand the intrinsic relation between magnetic fluctuations and density fluctuations experimentally requires simultaneous measurements of both in the core of a high-temperature plasma.

In this paper, we report on simultaneous multichord measurement of density and magnetic fluctuations using a three-wave interferometer-polarimeter system. Local density and magnetic fluctuation spatial profiles are deduced from line-averaged measurements by employing newly developed analysis techniques. Density fluctuation distributions for modes of specific helicity are found by selecting a test function with multiple free parameters to describe the spatial profile. The free parameters are varied to determine a best fit to the measured line integrals using a minimization procedure. The function fit and minimization routine approach, along with knowledge of local density fluctuations from interferometry, can also be used to model Faraday rotation fluctuation data from which one can determine the current density fluctuation, and hence magnetic field fluctuation spatial profile. Spatial structure for modes with $m=1$, $n=6$ to $n=8$ are identified.

II. INTERFEROMETER-POLARIMETER SYSTEM

A high-speed three-wave polarimeter-interferometer system has been developed to simultaneously measure the equi-

librium magnetic field and electron density profiles.⁵ The radiation source consists of three far-infrared (FIR) cavities (wavelength $\lambda_0=0.432$ mm) pumped by ~ 100 W of infrared CO₂ laser radiation. FIR cavities are slightly detuned to provide frequency offsets in the range of 1–2 MHz. The two probe beams are circularly polarized (R and L waves), while the local oscillator bias to each detector is linearly polarized. The phase difference between the R and L waves provides a measure of the Faraday effect, while the average is used to extract the electron density. The system has 11 vertically viewing chords (~ 8 cm separation) providing line-integrated measurements throughout the plasma cross section. Details of the system layout have been previously described.^{4,6} Frequency offsets allow time resolution of up to 2 μ s, which is sufficient to measure the dominant tearing modes with frequency of 10–20 kHz in Madison Symmetric Torus (MST). The increase in phase noise when measuring density and Faraday rotation concurrently has little effect on measurements of equilibrium quantities and density fluctuations. However, it does have an impact on magnetic fluctuation measurements since the equilibrium Faraday rotation phase shift ($\sim 3^\circ$) is much smaller than the interferometer phase shift ($\sim 1000^\circ$). Cross-talk between different intermediate frequencies and harmonic products from the mixers is a likely source of this noise which is under active investigation.

III. EXPERIMENTAL MEASUREMENT

Measurement of magnetic and density fluctuations are made on the MST RFP, a circular cross sectional device with major radius $R=1.5$ m, minor radius $a=0.52$ m, discharge current $I_p \leq 600$ kA, line-average electron density $n_e \sim 1 \times 10^{19}$ m⁻³, and electron temperature $T_e \leq 1$ keV. Typical plasma discharges without current profile control display a sawtooth cycle. Measured quantities are ensembled over many reproducible sawtooth cycles so that fluctuating quantities with specific mode number can be obtained using correlation techniques. Herein, plasmas with current of 400 kA and density $n_e=10^{19}$ m⁻³ were investigated.

^{a)} Contributed paper, published as part of the Proceedings of the 17th Topical Conference on High-Temperature Plasma Diagnostics, Albuquerque, New Mexico, May 2008.

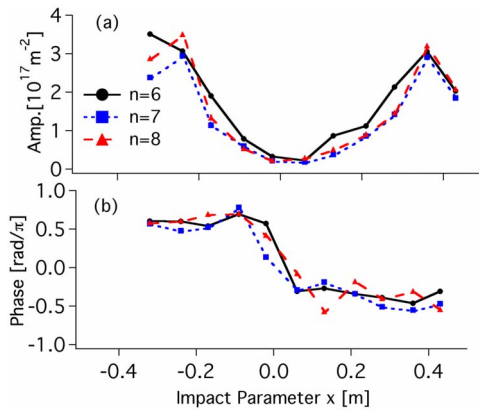


FIG. 1. (Color online) Line-integrated density fluctuation (a) amplitude and (b) phase for modes $m/n=1/6, 1/7, 1/8$.

The phase for line-integrated interferometry measurements is given by

$$\phi(x) = c_I \int_{-\sqrt{a^2-x^2}}^{\sqrt{a^2-x^2}} n_e(r) dz, \quad (1)$$

and that for polarimetry is given by

$$\psi(x) = c_F \int_{-\sqrt{a^2-x^2}}^{\sqrt{a^2-x^2}} n_e(r) \vec{B}(r) \cdot d\vec{z}, \quad (2)$$

where $c_I = e^2 \lambda / 4 \pi c^2 \epsilon_0 m_e$ and $c_F = e^3 \lambda^2 / 8 \pi^2 c^3 \epsilon_0 m_e^2$, and e , m_e , c , and ϵ_0 are electron charge, electron mass, light speed, and permittivity, respectively. In the above relations, x corresponds to the impact parameter and z is the distance along the chord. Each expression can be broken into mean and first order fluctuating quantities. The first order fluctuating quantities are given by

$$\tilde{\phi}(x) = c_I \int_{-\sqrt{a^2-x^2}}^{\sqrt{a^2-x^2}} \tilde{n}_e dz, \quad (3)$$

$$\tilde{\psi}(x) = c_F \int_{-\sqrt{a^2-x^2}}^{\sqrt{a^2-x^2}} [n_e \tilde{b}_z + \tilde{n}_e B_\theta \cos(\theta)] dz, \quad (4)$$

where θ is the angle between a FIR chord and the poloidal magnetic field. The fluctuating magnetic field \tilde{b}_z consists of both poloidal and radial components that vary with position along each chord.

Line-integrated density fluctuation measurements exhibit a hollow profile for each mode examined, as shown in Fig. 1(a). Data are from an ensemble of 130 sawtooth events at time 0.5 ms before a sawtooth crash. During the ensemble process, density fluctuations of specific helicity are isolated by correlating with data from external magnetic coil arrays. In the present case, poloidal (m) and toroidal (n) helicities of $m/n=1/6, 1/7, 1/8$ are selected and plotted versus impact parameter x . These correspond to the dominant core resonant modes. The density fluctuation amplitude gradually increases with impact parameter and has a minimum at the magnetic axis. Plasma density fluctuations correlated with magnetic fluctuations in MST result from plasma advection ($\tilde{n}_e = -\xi_r \nabla n_e$), where ξ_r is the plasma radial displacement. Effects of compression are considered negligible and therefore omit-

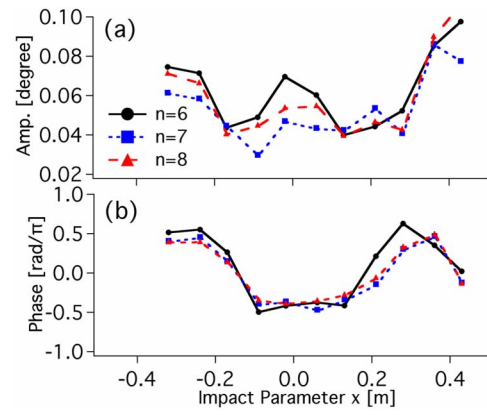


FIG. 2. (Color online) Line-integrated Faraday rotation fluctuation (a) amplitude and (b) phase for modes $m/n=1/6, 1/7, 1/8$.

ted in this treatment. Density fluctuations peak in the region of largest density gradient. For central chords ($x \rightarrow 0$), the interferometer is insensitive to density advection because the density profile is flat and the radial displacement is along the viewing line. Consequently, measured density fluctuations have a minimum on axis even though displacement has a maximum for $m=1$ mode.

Line-integrated density fluctuation phase with respect to radial magnetic field fluctuations at the plasma edge is plotted in Fig. 1(b) for modes with $m=1, n=6, 7, 8$. The phase for the inboard side is $\pi/2$, while that for the outboard side is $-\pi/2$. This identifies the odd, as opposed to even, nature of the $m=1$ density perturbation. When there is a density increase (decrease) for the inboard side, there is a corresponding density decrease (increase) for the outboard side, thus giving a π phase difference across the magnetic axis. The measured density perturbation is consistent with advection where the density fluctuation is in phase with radial displacement of the flux surfaces due to the magnetic perturbation. Radial magnetic field fluctuations with $m=1$ exhibit a $\pi/2$ phase shift with radial displacement for ideal plasmas.

Simultaneously measured Faraday rotation fluctuation profiles are shown in Fig. 2(a) for the same modes. Faraday rotation fluctuations are a combination of density and magnetic field fluctuations [see Eq. (4)], thereby requiring additional analysis to isolate each fluctuating quantity. Large amplitude fluctuations observed for the edge Faraday chords result primarily from density fluctuations [second term in Eq. (4)] which dominate chords with $x > 21$ cm and $x < -17$ cm. For $-17 \text{ cm} \leq x \leq 21$ cm, the second term in Eq. (4) is small due to the fact that the equilibrium poloidal magnetic field, $B_\theta(r)$, is nearly perpendicular to these chords and $m=1$. For these positions, magnetic fluctuations dominate the measurement according to the first term in Eq. (4).

The corresponding line-integrated phase between the various Faraday rotation chords and edge radial magnetic field fluctuations is shown in Fig. 2(b). For edge chords, both inboard and outboard, the phase difference is near $\pi/2$, while for central chords the phase is approximately $-\pi/2$. Unlike the interferometer measurements, there is no π phase change across the magnetic axis. Line-integrated phase near the edge will resemble that measured for density fluctuations

due to the density fluctuation dominance previously described, with the addition of a minus sign for the outboard side due to the $\cos(\theta)$ effect, as seen in Eq. (4). Near the plasma center, magnetic fluctuations determine the phase. To determine more accurately how each term in Eq. (4) contributes to the total phase, a new analysis procedure is necessary.

In order to evaluate the fluctuation-driven particle flux, local values for density fluctuation amplitude, magnetic fluctuation amplitude, and their relative phase are required. In an earlier work, the density fluctuation amplitude profile, but not phase profile, was obtained using an asymmetric Abel inversion technique.⁷ Herein, a new method is developed to obtain local profiles for density and magnetic field fluctuation amplitude and phase.

A radially symmetric test function with multiple free parameters is used to determine the local density and phase fluctuation profiles by finding the optimum fit to the measured line integrals. Line-integrated amplitude and phase are first generated from the test function and then compared to experimental measurements. The error between experiment and model is minimized using a chi-squared (χ^2) minimization technique to determine the free parameters. Measured density fluctuations, shown in Fig. 1(a), have a few characteristics of interest: the fluctuation amplitude on axis is a minimum and should have a maximum before going to zero at the wall. For $m=1$ mode, we have

$$\bar{\phi}(x) = C_I \int \tilde{n}_e(r) \cos \theta dz. \quad (5)$$

Moreover, $\bar{\phi}(x)$ must have a maximum at one location, that is, $\partial \bar{\phi}(x) / \partial x|_{x=x_1} = 0$. Therefore,

$$\frac{\partial \bar{\phi}(x)}{\partial x} = C_I \int \frac{\partial}{\partial x} \left(\frac{\tilde{n}_e}{r} x \right) dz = C_I \int \left[\frac{x^2}{r} \frac{\partial \tilde{n}_e}{\partial r} + \frac{\tilde{n}_e}{r} \right] dz = 0 \quad (6)$$

One specific solution of Eq. (6) is

$$\tilde{n}_e(r) = \tilde{n}_0 r \exp\left(-\frac{r^2}{2x^2}\right). \quad (7)$$

Considering the boundary condition $\tilde{n}_e(a)=0$, we choose a test function to fit line-integrated measurement of the form

$$\tilde{n}_e = \alpha_0 r^{\alpha_1} (1-r)^{\alpha_2} e^{\alpha_3 r^2}. \quad (8)$$

Through minimization, one can determine the four free parameters, α_0 , α_1 , α_2 , and α_3 , in Eq. (8), which provide the best fit.

By using this procedure, one can determine the local density fluctuation amplitude profile, as shown in Fig. 3(a), for the $m=1$, $n=6$, 7, and 8 modes. The inboard and outboard sides of the fluctuation are modeled separately to account for the differences between inboard and outboard mea-

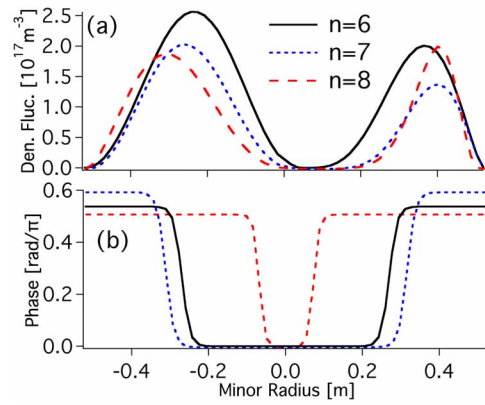


FIG. 3. (Color online) Local density fluctuation (a) amplitude and (b) phase for modes $m/n=1/6$, $1/7$, $1/8$.

surements. The Shafranov shift is included by using offset flux surfaces which vary from ~ 5 cm at the magnetic axis to zero at the boundary.

In the same manner, by using a different test function, the local density fluctuation phase profile with respect to b_r at the wall can be found, as shown in Fig. 3(b). The phase near the plasma outboard edge is $-\pi/2$, making a transition into $\pi/2$ at the inboard edge. The free parameters for modeling the phase affect the location of this transition and the rate at which it occurs. It has been observed that the choice for the modeled phase and density fluctuation profiles (i.e., test functions) affect the modeled line-integral profiles for both so that the determination of the local amplitude is coupled to the determination of the local phase.

Determining local profiles from the Faraday rotation fluctuation term is more demanding because of the existence of four unknown quantities in Eq. (4): equilibrium density, fluctuating $b(r)$, fluctuating $n_e(r)$, and equilibrium $B(r)$. The local density fluctuation profile must be determined first so that it can be used when inverting Eq. (4). Equilibrium density and poloidal magnetic field are obtained directly from measurements using the previously established techniques.⁵ This leaves only the fluctuating magnetic field to be modeled. Future work will focus on this topic.

¹P. C. Liewer, Nucl. Fusion **25**, 543 (1985).

²R. J. Bickerton, Plasma Phys. Controlled Fusion **39**, 339 (1997).

³J. M. Finn, P. N. Guzdar, and A. A. Chernikov, Phys. Fluids B **4**, 1152 (1992).

⁴W. X. Ding, D. L. Brower, D. Craig, B. H. Deng, S. C. Prager, J. S. John, and V. Svidzinski, Phys. Rev. Lett. **99**, 055004 (2007).

⁵B. H. Deng, D. L. Brower, W. X. Ding, M. D. Wyman, B. E. Champman, and J. S. Sarf, Rev. Sci. Instrum. **77**, 10F108 (2006).

⁶D. L. Brower, W. X. Ding, S. D. Terry, J. K. Anderson, T. M. Biewer, B. E. Chapman, D. Craig, C. B. Forest, S. C. Prager, and J. S. Sarf, Rev. Sci. Instrum. **74**, 1534 (2003).

⁷N. E. Lanier, D. Craig, J. K. Anderson, T. M. Biewer, B. E. Chapman, D. J. Den Hartog, C. B. Forest, S. C. Prager, D. L. Brower, and Y. Jiang, Phys. Plasmas **8**, 3402 (2001).